EXPERIMENTAL AND NUMERICAL INVESTIGATION ON THE CREEP CRACK GROWTH IN IN718

A. Lo Conte
Department of Mechanical Engineering, Politecnico di Milano, Milano, Italy

ABSTRACT

Creep crack growth (CCG) behaviour of Inconel 718 superalloy are investigated by means of experimental tests and numerical simulation at the temperature of 687 °C. The CCG tests are carried out with different initial values of the stress intensity factor on a standard compact-tension specimen. Creep crack growth are simulated using the finite element code ABAQUS and creep constants obtained from creep tests. C* parameter is used for characterizing CCG behaviour under the steady-state condition. Experimental and numerical results will be compared. Moreover Nikbin, Smith and Webster approach, for the evaluation of the time of crack initiation and the rate of damage accumulation, will be assessed.

1 INTRODUCTION

The Ni-based alloy Inconel 718 (IN718) is widely used in high temperature applications due to its highly satisfactory price/overall performance ratio.

High temperature structural components are often subjected to non-uniform stress and temperature distribution during service. These conditions may cause localized creep damage in the form of service initiated cracks which can propagate and ultimately cause fracture. Therefore, there is considerable interest in developing the technology for predicting creep initiation and creep crack growth behaviour.

In this paper , creep crack growth behaviour of Inconel 718 superalloy is investigated by means of experimental tests and numerical simulation at the temperature of 687 °C. For determining material constant to calculate the fracture parameters and to carry out numerical simulation, creep tests are conducted with various applied loads at the same temperature of the creep crack growth tests.

So far, several crack tip parameters have been proposed for characterizing crack growth at high temperature (Schwalbe et al. [1], Tabuchi et al. [2]). In this paper C* parameter is used for characterizing CCG behaviour under the steady-state condition. Moreover, the Nikbin, Smith and Webster approach [3], is used to assess the time of crack initiation and the rate of damage accumulation.

2 MATERIAL

The material used in this study is a commercial prepared Inconel 718 nickel superalloy, hot worked by forging in a 150 mm diameter bar, and having material composition listed in table l.

The heat treatment consisted of two hours at 1025 °C followed by water quenching, then six hours at 780°C followed by air cooling. The mechanical properties a t 687 °C are reported in table 2.

C	Si	Mn	P	S	Cr	Mo	Ni	Al	B
0.032	0.16	0.1	0.006	0.001	17.26	2.98	50.86	0.55	0.003

Co	Cu	Nb	Ti	Se	Ta	Fe	Pb	Bi
0.08	0.03	5.15	1.03	1ppm	0.007	bal.	1ppm	3ppm

Table 1 Chemical Composition of Inconel 718.

E [MPa]	ν	$\sigma_{p,0.2}$ [MPa]	σ_U [MPa]
158000	0.29	792	965

Table 2 Mechanical properties of Inconel 718 at 687 °C.

3 CREEP CRACK GROWTH TESTS

The specimen used for crack growth tests is the standard compact tension (CT) specimen configuration is shown in figure 1. The crack plane is parallel to the hot working direction and the crack grew in the radial direction. The CT specimens are fatigue pre-cracked, at room temperature, under constant amplitude loading, R=0.05, with maximum load equal 6.5 kN. The fatigue pre-cracks are between 2 and 4 mm from the notch root. Three samples were tested at 687 °C on a Satec constant load creep machines with a lever arm ratio of 20:1. During the tests crack growth measurements were made by the electrical potential technique. A current of 10 A was used. The output voltage was converted to crack length using an experimental calibration curve previously developed by the author. After crack growth testing, the CT specimen was fractured and then the final crack length was measured. When the actual final crack length was different from the measured on by the potential method, the measured crack length was adjusted. Also, the crack opening displacements at the load line (pin centre to centre) were measured with two linear variable displacement transducers (LVDTs) .

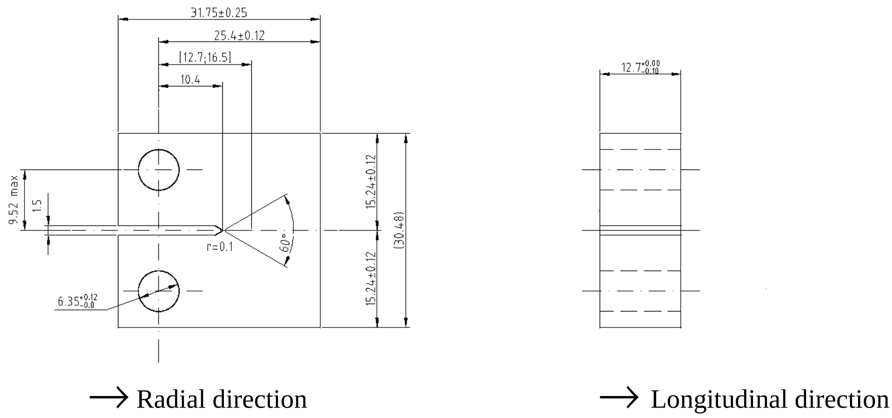

Figure 1 Compact Tension specimen configuration used for crack growth tests, dimensions in mm.

Fracture surface of the Compact Tension sample tested with K_I equal to 22 MPa $m^{1/2}$ is shown in figure 2 where the extension of the fatigue propagation, the extension of the creep crack growth and the final brittle rupture, are also indicated. The relationship of crack length versus time at 687 °C obtained in this tests are shown in figure 3, for three different initial values of K_I. The test carried out with K_I equal 22 MPa $m^{1/2}$ has been interrupted after 116 hours.

The value of crack initiation can be defined as corresponding to Δa = 0.2 mm (Schalbe et al. [1]) and the initiation time can be obtained directly by the potential drop measurement as reported in table 3. For the non interrupted tests, it can be observed that the initial transition crack growth stage occupied about 20 % of life, the constant crack growth rate period occupied about 50% of life and accelerating crack growth occupied about 30% of life. Hence, the constant rate period occupied a large part and the accelerating period occupied a small part of the rupture life. The increase of creep crack during the constant rate period was small and crack grew rapidly during the acceleration stage. The values of creep crack extension rate during the stationary period are reported in table 3.

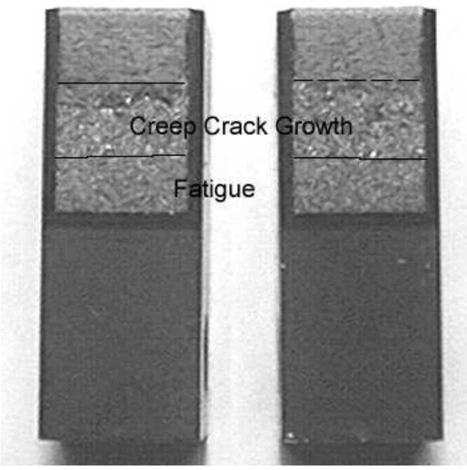

Figure 2 Fracture surface of sample tested with K_I = 22 MPa $m^{1/2}$.

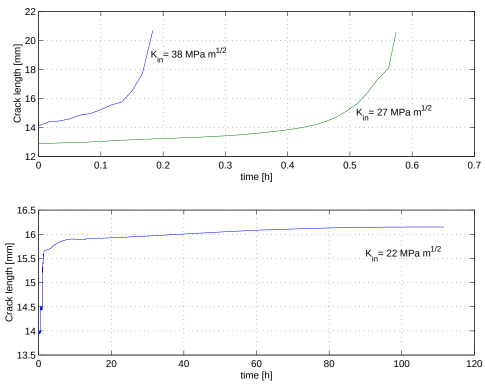

Figure 3 Creep crack length versus time for three different initial values of K_I.

K_I [MPa $m^{1/2}$].	22	27	38
t_i [h]	5.7	0.12	0.02
da/dt [mm/h]	1.05 10^{-3}	1.67	11.91

Table 3 Initiation time and stationary creep crack extension rate.

Figure 4 shows the relationship of load line displacement versus time at 687 °C, obtained for the three examined initial values of K_I. After the displacement due to the load application, a primary creep type behaviour prevail during same portion of the initiation time, manifesting in the form of decreasing displacement rate with time. The crack tip opening displacement at initiation time can be obtained from load line displacement and is also reported in table 3.

For extension following initiation, it is usual relate creep crack extension rate to a fracture mechanics parameter C^*. For tests carried out with constant applied load F, the C* parameter is determined using the expression provided in ASTM E1475. the results are reported in figure 5

On the basis of the obtained results more CCG test, with values of K_I. that allow a slow crack growth, are planned. Moreover, test on Inconel 718 superalloy with different heat treatment will be carried out.

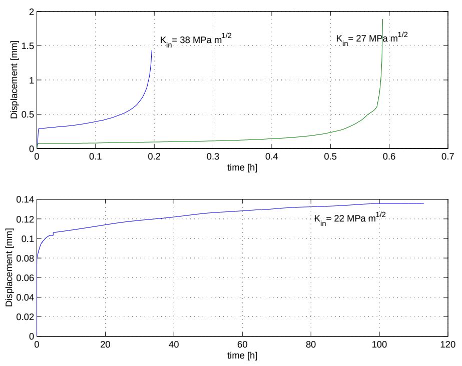

Figure 4 Load line displacement versus time.

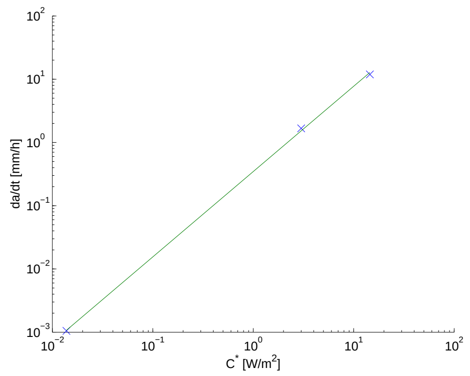

Figure 5 Creep crack growth extension rate versus C*.

4 CREEP PROPERTIES

Creep tests were carried out in the same Satec System used for CCG tests. Uniaxial tension creep experiments were performed in air at the temperature of t 687 °C and at the initial applied stress levels ranging from 540 to 610 MPa (figure 6). The samples have been machined in the radial direction of the bar, in order to reproduce the creep behaviour perpendicularly to the crack plane. The temperature of the sample was controlled by means of three thermocouples on the gauge length to ±0.5 °C of the set point. Creep strain measurements were obtained using an LVDT extensometer attached to the end sections of the specimen gauge length.
An average creep rate, obtained directly from the creep rupture data, has been evaluate to account for all three stages of creep. This average creep rate is defined by

$$\dot{\varepsilon}_A = \frac{\varepsilon_f}{t_r} = \dot{\varepsilon}_0 \cdot \left(\frac{\sigma}{\sigma_0}\right)^{n_A} = A \cdot \sigma^{n_A} \qquad (1)$$

where ε_f is the uniaxial failure strain, t_r is the time to rupture and σ is the applied stress.
The material constant A_A and n_A have been obtained from the results shown in figure 7. These data will allow an evaluation of the time of crack initiation and the rate of damage accumulation, according the Nikbin, Smith and Webster approach (Nikbin et al [3]), and are also used for numerical analysis described in the following section.

5 FINITE ELEMENT SIMULATION

Crack growth in the experimentally tested CT specimens will be simulated by means of the finite element code ABAQUS. The crack is assumed to grow constantly from the experimental initial value to the final one, under the external load (Zhao et al. [4], Yatomi et al. [5]).

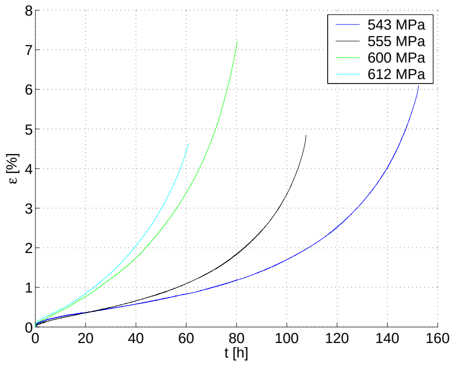

Figure 6 Creep curves for tests at 687 °C.

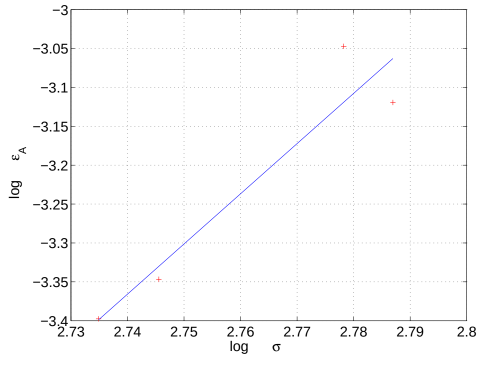

Figure 7 Average creep strain rate versus stress.

The mesh used for the analysis consists of about 6000 four-nodes plane strain isoparametric elements, as shown in figure 8 for the specimen tested at K_I.= 27 MPa m$^{1/2}$, where an extremely dense mesh was generated around the crack growth area.

Only the upper half of the specimen is considered due to the symmetry. The load is applied to a rigid pin constructed to fit the hole as shown in the mesh. The rigid pin and the specimen were modelled as contact surfaces. Crack growth is simulated by releasing a sequence of 180 nodes along the lower boundary of the dense portion of the mesh.

A criterion of crack length versus time is given to control the crack growth procedure, i.e., the debonding of the 180 nodes from the rigid surface. As the crack growth from one nodal position to the next, the force carried by the node is gradually released over a number of time increments.

Calculations are performed using elastic-plastic-creep behaviour. As discussed in the previous section, the creep response is described by a secondary creep law using the average creep properties. The plastic response is assumed to be governed by a Mises flow rule with isotropic hardening. Full account is taken in the analysis for large displacement and rotation.

During the crack growth analysis, the load-line displacement is recorder as function of the time and subsequently used to calculate the parameter C*. The FE results will be compared with the experimental one.

Moreover, the evolution of the creep damage behind the current crack tip will be examined, a preliminary results is shown in figure 9, and crack tip stress field will be investigated at different stages of crack growth.

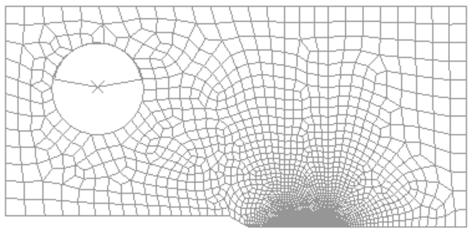

Figure 8 Finite element mesh..

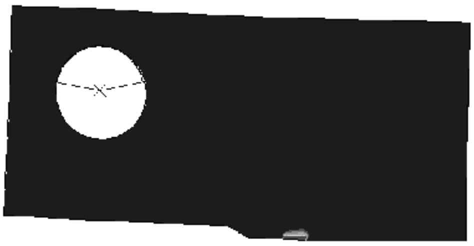

Figure 9 Evolution of the creep zone.

REFERENCES

[1] Schwalbe K. H., Ainsworth R. A., Saxena A. and Yokobory T., “Reccomendation for a Modification of ASTM E1457 to Include Creep-Brittle Materials”, *Engineering Fracture Mechanics*, Vol. 62, pp. 123-142, 1999.

[2] Tabuchi M., Kubo K., Yagi K., Yokoboki A. T. and Fuji A., “Results of a Japanese Round Robin on Creep Crak Growth Evaluation Methods for Ni-Base Superalloys”, *Engineering Fracture Mechanics*, Vol. 62, pp. 47-60, 1999.

[3] K. M. Nikbin, D. J. Smith, G. A. Webster, An Engineering Approach to the Prediction of Creep Crack Growth, Journal of Engineering Materials and Technology, Vol. 108, pp. 186-191, 1986.

[4] Zhao L. G., Tong J., Byrne J., Finite Element Simulation of Creep Crack Growth in a Nickel Base Superalloy, Engineering Fracture Mechanics, vol 68, pp.. 1157-1170, 2001.

[5] Yatomi M., Nikbin K. M., O’Dowd N. P., Creep Crack Growth Prediction Using a Damage based Approach, *International Journal of Pressure Vessels and Piping*, vol. 80, pp.. 573-583, 2003.

[6] Jianting G., Ranucci D., Picco E. and Strocchi P.M., “An Investigation on the Creep and Fracture Behavior of Cast Nickel-Base superalloy IN738LC”, *Metallurgical Transactions A*, Vol.14A, pp. 2329-2335, 1983.

[7] Tian S.G., Zhang J. H., Zhou H. H., Yang H. C., Xu Y. B. and Hu Z. Q., “Creep Behaviour of Single Cristal Nickel Base Superalloy”, *Material Science and Technology*, Vol. 14, pp. 751-756, 1989.

[8] Andersson H., Perrson C.,and Hansson T. “Crack Growth in IN718 at High Temperature”, *Internationl Journal of Fatigue.*, Vol. 23, pp. 817-827, 2001.

[9] Wanhill R.J.H., “Significance of Dwell Cracking for IN718 Turbine Discs”, *Internationl Journal of Fatigue*, Vol. 24, pp. 545-555, 2002.